Optica Applicata, Vol. XVI, No. 2, 1986

Variable wavelength interferometry III. Reflected-light techniques *

MAKSYMILIAN PLUTA

Central Optical Laboratory, ul. Kamionkowska 18, 03–805 Warszawa, Poland.

This paper follows two other ones which dealt with a new interferometric method – the variable wavelength interferometry (VAWI). In the previous papers the transmitted-light techniques have been presented, now those for reflected light are described. Measuring examples using simultaneously transmitted- and reflected-light versions of the VAWI techniques are also given.

1. Introduction

In two previous papers [1], [2], the fringe-field and uniform-field techniques of the variable wavelength interferometry (VAWI) have been presented for using in transmitted light. Now, these techniques are extended for reflected-light interferometry.

Reflected-light interference systems apply to objects whose surfaces reflect light. When the object to be studied is opaque or transparent but relatively thick (much thicker than the wavelength of incident light), then only rays reflected from the object surface faced the incident light are primarily responsible for interference patterns. If the object is surrounded by an air medium, no significant refractive index dispersion effects are created by it, and interference orders can be identified easier than those in transmitted light interference patterns; however, different phase jumps of light reflected at surfaces of different materials produce some problems for the reflected-light VAWI techniques.

2. Principle

Let an object O be attached to a substrate S (Fig. 1) and placed in the object plane of a light-reflecting two-beam interferometer adjusted to fringe-field interference in the image plane. Suppose that the object is a plate-like stripe of thickness t. We assume that a parallel beam of monochromatic light strikes the object O and its substrate S. Part of incident light is reflected back from O and S,

* This work was carried out on the Research Project PR–3.20.

and an optical path difference (δ) arises between reflected rays R′ and R. If the object is surrounded by air, then

$$\delta = 2t + \delta_j, \tag{1}$$

where δ_j is the additional path difference due to different phase jumps (ψ and ψ') on reflection for rays R and R′, i.e.

$$\delta_j = \frac{\lambda}{2\pi}(\psi' - \psi) = \frac{\lambda}{2\pi}\Delta\psi. \tag{2}$$

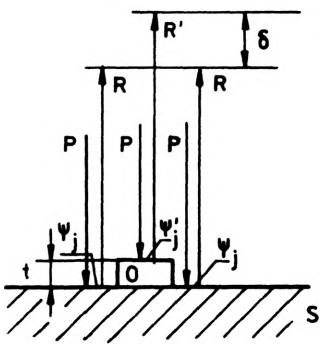

Fig. 1. Light-reflecting object O of thickness (height) t on a light-reflecting substrate S. P – parallel rays of incident light beam, R and R′ – reflected rays, δ – optical path difference between rays R′ and R

If ψ' is greater than ψ, δ_j is positive and, vice versa, δ_j is negative if $\psi' < \psi$. When the object and its substrate are of the same material, the phase jumps ψ' and ψ are identical, and $\delta_j = 0$. Note that ψ' and ψ in Eq. (2) are expressed in radians.

It is well known the fact that the interfringe spacing (b) varies with light wavelength (λ). This variation manifests itself as the movement of interference fringes toward the fringes of low interference orders (Fig. 2a) when λ becomes shorter and shorter, and, vice versa, the movement of fringes is from the low order fringes when λ becomes longer and longer (Fig. 2c). Consequently, starting from a long or short wavelength permits us to select such a particular wavelength λ_1 (Fig. 2b) for which the interference fringes (I′) displaced by the object under study occupy the positions coincident with those of fringes (I) produced by light reflected from the substrate. Such a situation is always possible if the optical path difference δ produced by the object O (Fig. 1) is not too small, say, $\delta > \lambda$.

One of the basic purposes of any interferometer is to measure precisely the optical path differences. Normally, this measurement is possible if the orders of interference fringes are known. In general, the order of a given interference fringe in the image of an object under study cannot exactly be identified if there are no continuous and easily distinguishable connections between deflected and undeflected fringes (I′ and I, Fig. 2). This drawback can be overcome by using the VAWI method, which does not need to identify the position of the interference fringe of the zero (or other) order, but it requires merely to determine the number of interfringe spacings b by which fringes (I′) in the image of the object under

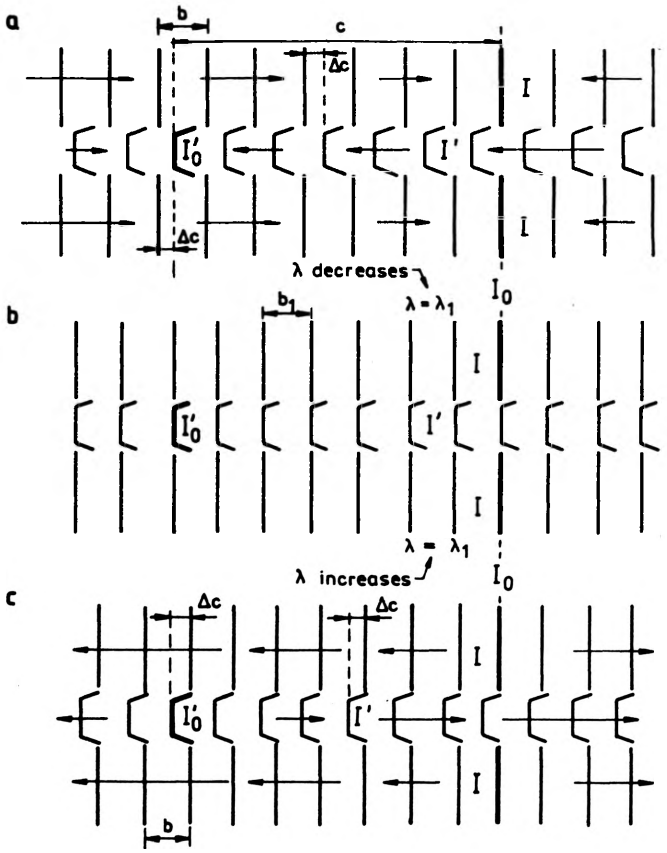

Fig. 2. Schematic reflected-light interferograms of an object of uniform height as shown in Fig. 1. I and I′ – interference fringes produced by light reflected, respectively, from the substrate (S, Fig. 1) and the object (O). I_0 and I'_0 – hypothetical fringes of the zero interference order

study are displaced with respect to reference fringes (I) of the same interference orders. The reference fringes are those produced by light reflected from the substrate (S, Fig. 1).

It is clear that the situation shown in Fig. 2b can mathematically be expressed as

$$\delta_1 = 2t + \delta_{j1} = m_1 \lambda_1, \tag{3}$$

where m_1 is the above-mentioned number of interfringe spacings by which the object displaces the interference fringes produced by light of wavelength λ_1. In this case the number m_1 is an integer and is called the initial or introductory interference order. Similarly, the situations shown in Figs. 2a and 2c may be described as

$$\delta_2 = 2t + \delta_{j2} = (m_1 + q_2)\lambda_2, \tag{4}$$

where q_2 is a fraction number or an integer, which expresses the increment or the decrement of the interference order with respect to m_1 when the wavelength of light is changed from λ_1 to λ_2. If λ_2 is longer than λ_1, the quantity q_2 is negative

and, vice versa, it is positive if $\lambda_2 < \lambda_1$ as shown, respectively, in Fig. 2a and Fig. 2c. From Eqs. (3) and (4) it follows that

$$m_1 = q_2 \frac{\lambda_2}{\lambda_1 - \lambda_2} + \frac{\delta_{j1} - \delta_{j2}}{\lambda_1 - \lambda_2} \tag{5}$$

or

$$m_1 = q_2 \frac{\lambda_2}{\lambda_1 - \lambda_2} + \frac{(\Delta\psi)_1 \lambda_1 - (\Delta\psi)_2 \lambda_2}{2\pi(\lambda_1 - \lambda_2)} \tag{6}$$

where, in accordance with Eq. (2), $\delta_{j1} = (\Delta\psi)_1 \lambda_1/2\pi = \lambda_1(\psi'_1 - \psi_1)/2\pi$, and $\delta_{j2} = (\Delta\psi)_2 \lambda_2/2\pi = \lambda_2(\psi'_2 - \psi_2)/2\pi$. If there is no spectral dispersion of the phase jumps, $(\Delta\psi)_1 = (\Delta\psi)_2 = \Delta\psi$ and Eq. (6) takes the form

$$m_1 = q_2 \frac{\lambda_2}{\lambda_1 - \lambda_2} + \frac{\Delta\psi}{2\pi}. \tag{7}$$

When the object under study (O, Fig. 1) and its substrate (S) are of the same material, the difference $\Delta\psi$ of phase jumps is equal to zero and the above equation reduces simply to

$$m_1 = q_2 \frac{\lambda_2}{\lambda_1 - \lambda_2}. \tag{8}$$

In general, $\Delta\psi$ is much smaller than unity for different combinations of two common materials. If, for instance, the object O (Fig. 1) is an aluminium stripe on a glass substrate, $\Delta\psi \approx -0.07$ for the middle region of the visible spectrum. Consequently, the initial interference order can be determined from Eq. (8) for many combinations of two different materials; the value obtained from this equation should only be accepted for further calculations as the nearest integer. If, for instance, it follows $m_1 = 6.9$ from Eq. (8), then in reality m_1 is equal to 7.

If the optical path difference δ is several times greater than λ, the increment q_2 may be as great as 0.5, 1, 1.5, 2, 2.5, 3, and even more. In this case Eq. (4) can be developed into several further equations, and we can write

$$\delta_1 = 2t + \delta_{j1} = m_1 \lambda_1, \tag{9a}$$

$$\delta_2 = 2t + \delta_{j2} = (m_1 + 0.5)\lambda_2, \tag{9b}$$

$$\delta_3 = 2t + \delta_{j3} = (m_1 + 1)\lambda_3, \tag{9c}$$

$$\delta_4 = 2t + \delta_{j4} = (m_1 + 1.5)\lambda_4, \tag{9d}$$

. . . . . .

. . . . . .

for $\lambda_1 > \lambda_2 > \lambda_3 > \lambda_4 \ldots$ if λ_1 is selected in the long-wave (red) region of the visible spectrum. The above family of equations enables the initial interference order m_1 to be calculated from different combinations of two Eqs. (9a) and (9b), (9a) and

(9c), (9a) and (9d), ..., (9b) and (9c), (9b) and (9d), ..., (9c) and (9d), and so on. A mean integer value m_1 is then taken for determining optical path differences $\delta_1, \delta_2, \delta_3, \ldots$. The increments $q_2 = 0.5$, $q_3 = 1$, $q_4 = 1.5$, ... which are in Eqs. (9b), (9c), (9d), ... can be evaluated visually without any measurment as shown earlier [1, 2].

The above considerations refer to both fringe-field and uniform-field interferometry. There is no difference between the two techniques at their theoretical level. However, some nuances occur between them when they are put into practice.

The situation described by Eqs. (9) requires only to know or measure the wavelengths $\lambda_1, \lambda_2, \lambda_3, \ldots$ for determining the optical path differences $\delta_1, \delta_2, \delta_3, \ldots$. Otherwise, if the increments q cannot be equal to 0.5, 1, 1.5, 2, ..., they must be measured very precisely. Both the fringe-field and uniform-field VAWI techniques are therefore suitable especially for the study of objects which produce high order interference patterns.

3. Practical implementation

A double-refracting interference microscope – the same Biolar PI as in two previous experiments [1], [2] – has been used for the verification of the above-presented theoretical considerations. Only an epi-illuminator with a wedge interference filter has been attached to the microscope body (Fig. 3). A detailed description of this reflected-light version of the double-refracting interference system is ignored here since it may be found in [3]. However, it is worth while to note the fact that the system incorporates three combinations of two simultaneously acting birefringent prisms (Fig. 4): 1) W_0+W_1, 2) W_0+W_2, and 3) W_0+W_3. The first and third combinations are for uniform-field interferometry, while the second is for fringe-field interferometry. The prism W_0 is installed in microscope objectives and can be rotatable about the optic axis of the objective. The rotation is for changing the amount and direction of wavefront shear. The interchangeable prisms W_1, W_2, and W_3 are installed in a turret inside the microscope head at a proper (controlled) distance behind the objective Ob. They are translated transversely (p) to the objective axis by means of a micrometer screw PS referred to as tha phase screw. This translation permits the interfringe spacings b (hence the wavelengths λ) and increments or decrements q of the initial interference order m_1 to be measured. The results of measuremet are reading on the scale of the micrometer screw PS. The relation between b and λ is the same as for transmitted light [4], but the value of b for a given wavelength λ is now reduced by a factor equal exactly to 2. This reduction is caused by twofold passage of light waves through birefringent prisms.

The passage of light waves from a source (LS, Fig. 4) to the object under study, via the birefringent prisms, gives rise to a phase difference between sheared wavefronts incident on the object O. But, for backwards wavefronts the phase

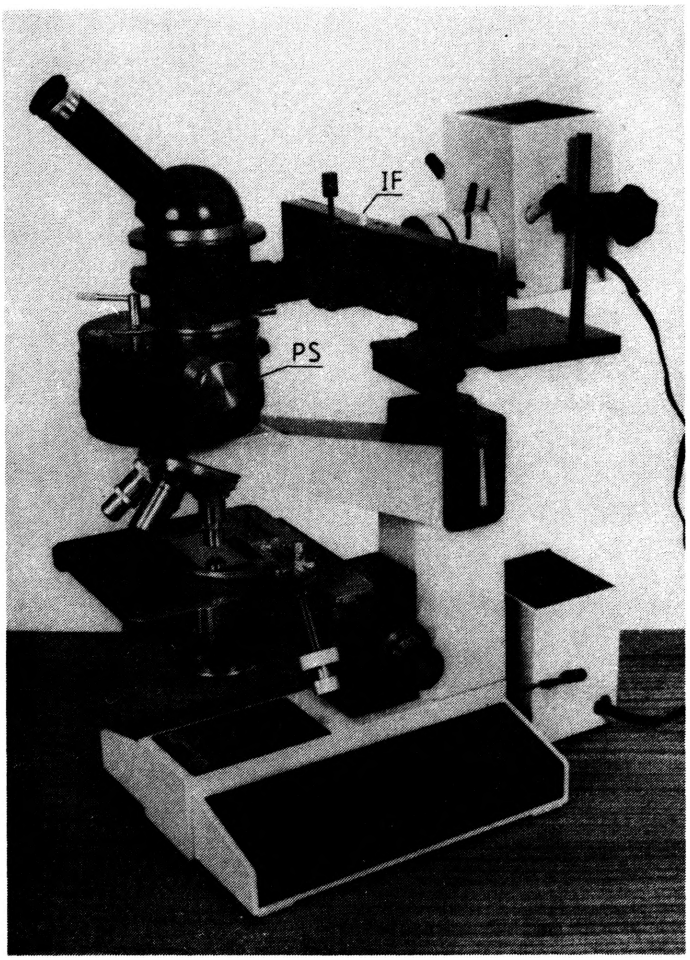

Fig. 3. Double-refracting interference microscope Biolar PI fitted with an epi-illuminator. IF – wedge interference filter, PS – micrometer screw (phase screw), by means of which interfringe spacings b (Fig. 2) and decoincidences Δc of deflected (I') and undeflected (I) interference fringes are measured

difference produced by these prisms is of opposite sign, and the resultant phase difference is equal to zero in the exit pupil of the objective. Consequently, no interference fringes are observed in this pupil, and the interfringe spacings b cannot be measured, when the uniform-field VAWI technique comes into question, with the use of the procedure suggested earlier for transmitted-light VAWI method [2]. Now, the half-shade procedure [4] or "balancing" procedure is recommended. The latter is based on identical (balanced) appearance of totally sheared images of a single isotropic object observed against the maximally dark background (Figs. 5a and c); the object mentioned may be that which is currently measured. To use this technique the polarizer P (Fig. 4) and analyser A are crossed and the birefringent prism W_1 or W_3 is first set so that the background of the field of view appears maximally dark in zero interference order (Fig. 5a), and then this prism is translated in the transverse direction (p) until the background appears maximally dark for the second time (Fig. 5c). The translation of the prism from the first

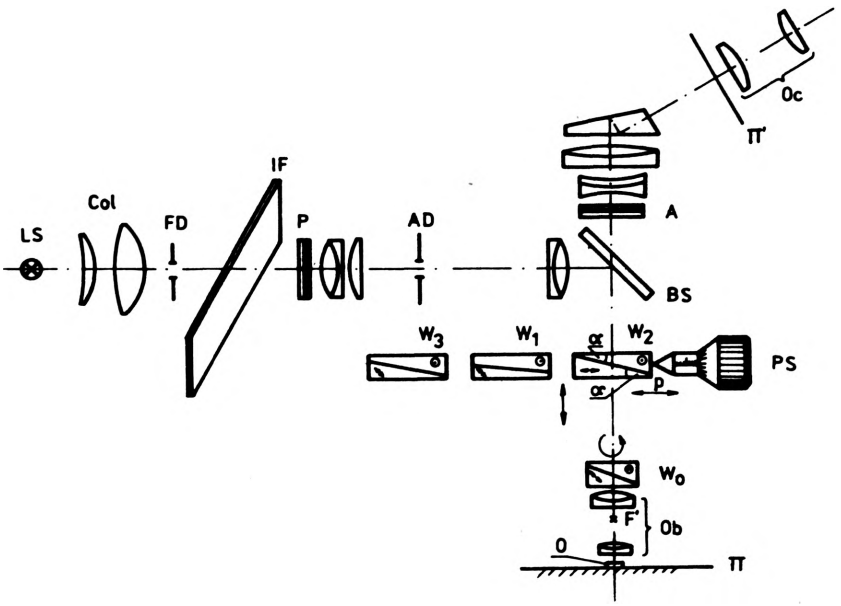

Fig. 4. Basic optical components of the interferometer shown in Fig. 3. LS – source of white light (halogen lamp 12V/100W), Col – collector, FD – field diaphragm, IF – wedge interference filter, P – polarizer, AD – aperture diaphragm, BS – beam splitter (semi-reflecting plate), W_1, W_2 and W_3 – interchangeable birefringent prisms, Ob – objective with birefringent prism W_0 (its own interference fringes are in coincidence with the back focal point F′ of the objective), O – object under study, Π – object plane of the objective Ob, A – analyser, Π′ – image plane of the objective Ob, Oc – ocular, PS – micrometer screw (phase screw), by means of which the birefringent prisms W_1–W_3 are moved in the transverse direction (p)

position p_1 (Fig. 5a) to the second p_2 (Fig. 5c) expresses simply the interfringe spacing b for the uniform-field interferometry. However, the observer has some difficulties in the correct visual estimation of the maximum darkness of the background. This defect is overcome if the positions p_1 and p_2 are fixed at such points for which the left-hand and right-hand images of the object under study appear to be identical. This criterion is extremely sensitive to incorrect positions p_1 and p_2 of the birefringent prism, and a quite small deviation from them manifests itself as a significant loss of identity of both images (Fig. 5b). It is clear that this way permits us also to measure a multiple value of b, say $10b$, in order to obtain extremely accurate value for a single interfringe spacing.

Where the fringe-field light-reflected VAWI technique is concerned, the interfringe spacings are measured in a way described earlier for transmitted light [1].

The twofold passage of light waves through birefringent prisms (Fig. 4) allows a pupil phase-difference autocompensation to be achieved, thus an extended light source without any slit diaphragm can be used. The interference system works satisfactorily with an ordinary epi-illuminator, which incorporates an aperture

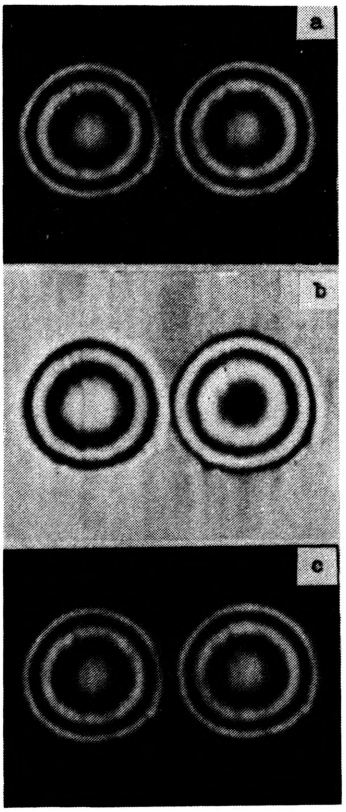

Fig. 5. "Balancing" method of the measurement of the interfringe spacing in uniform-field interferometry. (a) and (c) – two succesive balancing positions of the birefringent prism W_3 (or W_1, Fig. 4), (b) unbalanced position of this prism

diaphragm (AD) and field diaphragm (FD), enabling one to obtain the correct Köhler principle of illumination. However, the wedge interference filter (IF) requires to use a small opening of the diaphragm AD.

4. The reflected-light VAWI technique in combination with transmitted-light interferometry

Let a transparent object O of thickness t (Fig. 6) be taken into consideration. We assume that no difference in phase jumps occurs between rays R′ and R reflected from the object O and its transparent substrate S (Fig. 6a). Thus, optical path difference between these rays is simply given by

$$\delta_R = 2tn' \tag{10}$$

where n' is the refractive index of the medium which surrounds the object O. Next, let this object be transilluminated as shown in Fig. 6b. Now, the optical path difference δ_T between rays T′ and T passing through the object O and its surround is expressed by

$$\delta_T = (n-n')t. \tag{11}$$

Combining Eqs. (10) and (11) yields

$$\delta_R = 2\delta_T \frac{n'}{n-n'}. \tag{12}$$

As can be seen, the optical path difference in reflection (δ_R) is always greater than that in transillumination (δ_T) if $n'/(n-n')$ 0.5. When the object is surrounded by air, $n' = 1$ and Eq. (12) takes the form

$$\delta_R = \frac{2}{n-1}\delta_T, \tag{13}$$

from which it follows that δ_R is always greater than δ_T if $n < 3$. This applies to almost all substances known in practice. If, for instance, $n = 1.5$, the optical path difference δ_R is 4 times greater than δ_T.

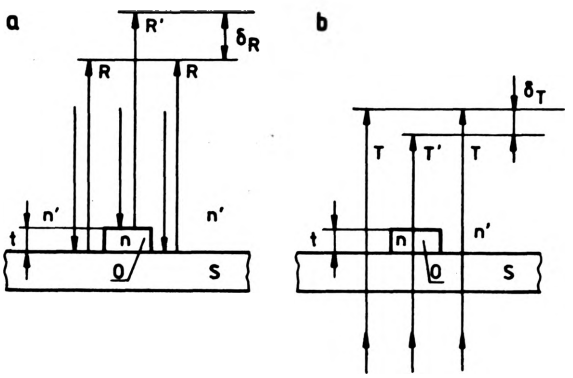

Fig. 6. Optical path differences, δ_R and δ_T, produced by a transparent object O and its transparent substrate S in reflected (a) and transmitted light (b)

From the above consideration it follows than the VAWI techniques are commonly more suitable for reflected light than for transmitted light so far as the favourable measuring situations with the interference order increment $q = 0.5$, 1, 1.5, 2, ... are important to a given interferometric problem.

Moreover, it is worth while to note that the reflected-light VAWI techniques combined with transmitted-light interferometry permit us to determine simultaneously the thickness t (from Eq. (10)) and the refractive index n (from Eq. (11)) of transparent objects.

5. Effect of the spectral dispersion of birefringence due to the double-refracting interference system

The ratio b/λ is among basic parameters of any interferometric system. The best interferometers are those for which this ratio is a constant or only slightly wevelength-dependent quantity. All double-refracting interferometers suffer from the spectral dispersion of birefringence of a material (e.g., quartz crystal) of which

the interference system is made. This defect causes the ratio b/λ to be not constant and thus the zero order interference fringe (I_0, Fig. 2) deflected by the object under study to be coloured in white light if the optical path difference δ introduced by the object to the interference field exceeds a particular value δ_a referred to as "achromatic".

In general, the optical path difference δ is expressed by

$$\delta = \frac{\lambda}{b} c \tag{14}$$

where λ is the wavelength of light used, b is the interfringe spacing (Fig. 2), and c is the distance between the deflected and undeflected fringes, I'_0 and I_0, of the zero interference order. The fringe I'_0 is achromatic in white light only when the distance c is identical for all wavelengths within the visible spectrum or, in other words, when the ratio b/λ is a constant parameter. This does not apply to the double-refracting interference systems.

Let λ_F and λ_C be the wavelength of the spectral lines F and C ($\lambda_F = 486.1$ nm, $\lambda_C = 656.3$ nm). For a light-reflecting object such as shown in Fig. 6a, we can write

$$c_F = \delta_F \frac{b_F}{\lambda_F} = 2t \frac{b_F}{\lambda_F}, \tag{15a}$$

$$c_C = \delta_C \frac{b_C}{\lambda_C} = 2t \frac{b_C}{\lambda_C}. \tag{15b}$$

On the other hand, the interfringe spacings b_F and b_C are defined by

$$b_F = \frac{\lambda_F}{2D_F \tan\alpha}, \tag{16a}$$

$$b_C = \frac{\lambda_C}{2D_C \tan\alpha}*. \tag{16b}$$

Here α is the apex angle of the birefringent prism W_2 (or W_1 and W_3, Fig. 4), and D_F and D_C are the double-refracting powers of the birefringent prism for λ_F and λ_C, respectively. If this prism is a typical Wollaston prism, $D_F = 2(n_{eF} - n_{oF})$ and $D_C = 2(n_{eC} - n_{oC})$, where n_{eF}, n_{eC} and n_{oF}, n_{oC} are the extraordinary and ordinary refractive indices of the birefringent prism.

By combining Eqs. (15) and (16) we obtain

$$c_C - c_F = t\left(\frac{1}{D_C \tan\alpha} - \frac{1}{D_F \tan\alpha}\right). \tag{17}$$

This equation defines the chromaticity of the zero order interferece fringe I'_0 (Fig. 2) deflected by the object under study (in white light), due to the spectral

* For transmitted-light double-refracting interferometry the interfringe spacings b_F and b_C are two times greater (see [2]).

dispersion of birefringence of the double-refracting prism. Let a typical Wollaston prism be taken into consideration, the apex angle α of which is equal to 9°. The prism is made of quartz crystal, whose refractive indices are $n_{oF} = 1.54970$, $n_{eF} = 1.55899$, $n_{oC} = 1.54193$ and $n_{eC} = 1.55095$ (data after HARDY and PERRIN [5]). For these quantities Eq. (17) takes the form

$$c_C - c_F = 10t. \tag{18}$$

This applies aproximately to the birefringent prism W_2 of the microinterferometer Biolar PI used for reflected-light interferometry.

On the other hand, the prism W_2 produces in reflected light the interference fringes whose interfringe spacings for spectral lines C and F differ by $b_C - b_F \approx 30$ μm. In fact, such a difference makes the undeflected fringes of the first interference orders to be completely chromatic in white light. However, it has experimentally been stated that no chromatism of the deflected fringe of the zero interference order is perceived if $c_C - c_F \leqslant (b_C - b_F)/4$. Consequently, this fringe retains its achromatic appearance for visual observation if the height t of the object O (Fig. 6a) does not exceeds a particular value t_a defined by

$$t_a = \frac{1}{4}\frac{b_C - b_F}{10} = \frac{30}{40} = 0.75 \text{ μm}.$$

Otherwise, the deflected fringe of the zero interference order will be coloured in white light. It is clear, that for

$$t \geqslant \frac{b_C - b_F}{10} = \frac{30}{10} = 3 \text{ μm}$$

this fringe will be completely coloured in white light.

The above discussion shows that the zero order interference fringe deflected by the object under study can be indetified using the reflected-light version of the microscope Biolar PI and white light if the object height (or thickness) t is very small. Fortunately, a less critical requirement holds good for the transmitted-light version of this instrument. In this case, Eq. (18) takes the form

$$c_C - c_F = 10(n-1)t \tag{19}$$

where n is the refractive index of the object under study (O, Fig. 6b) immersed in air medium (it is supposed that spectral dispersion of n is very small). Consequently, we can define the "achromatic" thickness of the object studied in transmitted light as

$$t_a \leqslant \frac{1}{4}\frac{b_C - b_F}{10(n-1)} = \frac{60}{40(n-1)} \text{ μm}.$$

If, for instance, $n = 1.5$, $t_a \leqslant 3$ μm.

As can be seen from the above discussion, the VAWI technique is extremely useful and even indispensable to reflecting-light interferometry using the double-refracting interference systems.

6. Measuring examples

In order to illustrate the possibilities of the reflected-light VAWI techniques, two measuring examples are given below. The first (Fig. 7) illustrates the measurement of the depth t of the groove in a microréfractometric plate manufactured by C. Zeiss Jena as an accessory to the Peraval-interphako microscope. The groove depth was fixed by the manufacturer to be equal to 12.5425 ± 0.0063 μm. This plate was used as a test object for the double-refracting microinterferometer Biolar PI adapted to the reflected-light VAWI techniques (Figs. 3 and 4).

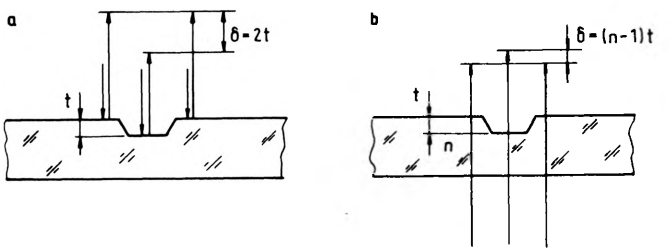

Fig. 7. Cross-section of the C. Zeiss (Jena) refractometric plate: (a) measurement of its groove depth t in reflected light, and (b) in transmitted light

The results of measurement in reflected light are given in Table 1. As can be seen, the value obtained for t is consistent with that given by C. Zeiss Jena. A small discrepancy between our result and the value given by the manufacturer is equal to 0.0077 μm and only slightly (by 0.0014 μm) exceeds the range of accuracy with which the groove was maesured in the C. Zeiss factory.

It is worth while to note that in white light an achromatic (black) fringe was observed among interference fringes deflected by the groove. However, the interference order of this achromatic fringe was heigher than zero, and in red light of wavelength $\lambda_1 = 660$ nm it was $35b_1$ away from the undeflected fringe I_0 (Fig. 2) of the zero interference order, whereas the true zero order deflected fringe I_0' was coloured in white light and located $38b_1$ away from I_0. This situation is consistent with the discussion given in Chapt. 5 of this article.

Additionally, the same groove (Fig. 7b) was measured by using the transmitted-light VAWI technique [1]. The results are listed in Table 2. As can be seen, the obtained value for the depth t is very well consistent with that given by the manufacturer. The dicrepany is, in this case, as small as 0.0021 μm, and it does not exceed the range of accuracy ($\Delta t = 0.0005\,t$) with which the depth of the groove was measured in the C. Zeiss factory.

The next measuring example concerns a lens-like droplet of Canada balsam. The same sample of the balsam was used as described earlier in [2]. Now, the height t and refractive index n of the droplet were measured by using both the reflected-light and transmitted-light uniform-field VAWI techniques. The results are listed in Table 3. As can be seen, the refractive index n for $\lambda = 553$ nm is very well

Table 1. Experiment with the C. Zeiss Jena refractometric plate by using the fringe-field reflecting-light VAWI technique: results of the measurement of the groove depth $t = 12.5425$ μm (this value was given by the manufacturer with an accuracy $\Delta t = 0.0005\,t$)

s	1	2	3	4	5	6	7	8	9	10		
q	0	1	2	3	4	5	6	7	8	9		
b [μm]	116.32	113.14	109.98	107.06	104.14	101.58	99.92	96.56	94.20	91.96		
λ [nm]	660.0	643.0	626.5	611.0	596.	583.0	574.0	556.5	544.0	532.0	Σm_1	$\bar{m}_1$
m_1	–	37.82	37.40	37.41	37.25	37.86	40.05	37.64	37.52	37.41	340.36	37.82
m_1	–	–	36.96	37.18	37.04	37.87	40.59	37.60	37.46	37.34	302.04	37.76
m_1	–	–	–	37.42	37.08	38.21	41.73	37.75	37.56	37.41	267.16	38.17
m_1	–	–	–	–	36.73	38.64	43.54	37.84	37.60	37.41	231.76	38.63
										$\Sigma m_1 = 1141.32$		
										$\bar{m}_1 = 38.04\ (= 38)$		
m	38	39	40	41	42	43	44	45	46	47		
δ [μm]	25.0800	25.0770	25.0600	25.0510	25.0320	25.0690	25.2560	25.0425	25.0240	25.0040		
t [μm]	12.5400	12.5385	12.5300	12.5255	12.5160	12.5345	12.6280	12.5213	12.5120	12.5020		
mean value of the groove depth $\bar{t} = 12.5348$ μm												

s – successive measuring situations, q – increments of the initial interference order m_1, b – interfringe spacings, λ – wavelengths corresponding with b, m – succesive interference orders, δ – optical path differences ($\delta = m\lambda$), $t = \delta/2$

Table 2. Experiment with the C. Zeiss Jena refractometric plate by using the fringe-field transmitted-light VAWI technique: results of the measurement of the same groove depth t as shown in Table 1

s	1	2	3	4	5	6	7	8	9	10	11	12
q	0	−0.5	+0.5	1	1.5	2	2.5	3	3.5	4	4.5	5
b [μm]	221.7	234.2	211.8	211.8	193.6	183.3	176.4	169.2	162.8	156.4	151.0	145.1
λ [nm]	639.5	673.5	611.5	587.0	565.0	537.0	519.5	500.5	484.0	467.0	453.5	435.5
n	1.5123	1.5114	1.5132	1.5142	1.5152	1.5167	1.5189	1.5189	1.5200	1.5213	1.5224	
m_1	–	9.90	10.92	11.18	11.37	10.48	10.82	10.80	10.89	10.83	10.97	10.67
from the above data it follows that $\bar{m}_1 = 10$, hence $m_1 = 10$												
m	10	9.5	10.5	11	11.5	12	12.5	13	13.5	14	14.5	15
δ [μm]	6.3950	6.3983	6.4208	6.4570	6.4975	6.4440	6.4938	6.5065	6.5340	6.5380	6.5758	6.5325
t [μm]	12.4829	12.5112	12.5112	12.5574	12.6116	12.4715	12.5435	12.5681	12.5654	12.5340	12.5876	–
mean value of groove depth $\bar{t} = 12.5404$ μm												

s, q, b, m_1, m and δ – as in Table 1, n – refractive indices of the refractometric plate, $t = \delta/(n-1)$

Table 3. Results of the measurement of the thickness t and refractive index n of a droplet of Canada balsam by using the uniform-field VAWI techniques for reflected light (measurement of t) and transmitted light (measuremet of n)

Reflected light							Transmitted light		
s	1	2	3	4	5	6	1	2	3
q	0	0.5	1	1.5	2	2.5	0	~0.5	~ −0.4
b [μm]	476.3	447.1	411.6	383.0	358.2	336.4	789.5	640.7	874.6
λ [nm]	662	623	577	538	504	477	553	456	675
m_1	–	8.50	6.80	6.50	6.40	6.50	–	2.25	2.21
	–	–	5.65	5.83	5.76	6.04	–	–	2.10
	–	–	–	5.90	5.90	6.20			
	–	–	–	–	5.75	6.32			
	–	–	–	–	–	6.83			
$\bar{m}_1 = 6.32$, i.e., $m_1 = 6$							$\bar{m}_1 = 2.19$, i.e., $m_1 = 2$		
m	6	6.5	7	7.5	8	8.5	2	2.5	1.6
δ [μm]	3.9720	4.0495	4.0390	4.0350	4.0320	4.0545	1.1060	~ 1.14	~ 1.08
t [μm]	1.9860	2.0248	2.0195	2.0175	2.0160	2.0273	–	–	–
			mean value of the thickness $\bar{t} = 2.01518$ μm						
n	–	–	–	–	–	–	1.5488	~ 1.56	~ 1.536

s, q, b, m_1, m, δ and t as in Table 1; $n = 1 + \delta/t$

consistent with that given previously in [2], whereas refractive indices for far red light and deep blue light are only roughly evaluated since the measuring situations were not favourable in these spectral regions.

7. Conclusions

It can be stated that both the fringe-field and uniform-field VAWI techniques function satisfactorily in reflected light and enable us to measure different objects in every respect and more accurately than by using standard interferometric procedures. The reflectedlight VAWI techniques are especially useful for interferometry based on double-refracting interference systems, such as the microinterferometer Biolar PI, which suffer from some spectral dispersion of double-refracting power.

Moreover, the reflected-light VAWI techniques permit the calibration of the interferometer to be performed very easily and accurately by using an extremely simple tool. This problem as well as the sensitivity and accuracy of the VAWI techniques will be discussed in a separate paper [6].

References

[1] PLUTA M., Optica Applicata **15** (1985), 375.
[2] PLUTA M., Optica Applicata **16** (1986), in the same volume.

[3] PLUTA M., Optica Acta **20** (1973), 625.
[4] PLUTA M., Optica Applicata **12** (1982), 19.
[5] HARDY A. C., PERRIN F. H., *The Principles of Optics*, McGraw–Hill Book Co., New York, London 1932.
[6] PLUTA M., *Variable wavelength interferometry*, Part IV (in preparation for publication in Optica Applicata).

Received January 22, 1986

Интерферометрия с плавно переменной длиной волны. III. Методы для отражённого света

Настоящая статья является продолжением двух предыдущих, говорящих о новом интерферометрическом методе (VAWI), в котором применяется переменную длину световой волны. В предыдущих статьях были описаны варианты этого метода для проходящего света, здесь, в свою очередь, представлен вариант для отражённого света. Даны также измерительные примеры с одновременным использованием метода VAWI в проходящем и отражённом свете.